structures have the general features shown in Figure 8. In particular, the angle around the transfering H^+ is between 155 and 165°, and the angle around the basic H^- is between 65 and 80°. There are substantial interactions between the Li^+ and the developing carbanionic center as indicated by the short C–Li distances (2.1–2.3 Å, except in TS3). Because this interaction involves the same developing orbital that the H^+ overlaps, the H–C–Li angle is smaller and its variation (47–56°) is smaller than the variation of the H–H–Li angle. The Li–N distance is relatively constant, also, unless a large separation of the carbanionic center and the nitrogen exists as in TS5, which prevents Li–N coordination.

Lithiation of Vinylamine by CH_3Li. The complexation energy for $H_2C{=}CH{-}NH_2 + CH_3Li$ was calculated to be 26 kcal/mol at the 3-21G level. The reaction barriers for α- and β-lithiation are 39 and 33 kcal/mol, respectively, as compared with the intrinsic barrier of 34 kcal/mol for the reaction of CH_3Li with CH_4.[28] As a model for intermolecular coordination, reaction of $CH_3Li{\cdots}NH_3 + CH_4$ was calculated at the 3-21G level. The energetics of these reactions are shown in Figure 9.

Because of the directionality of the CH_3–Li interaction, the H–CH_3–Li angles in the transition structures are smaller than those involving hydride as a base. The decrease of the H–CH_3–Li angle provides an opportunity for an increase in the CH_3–H–C angle, and a better collinear arrangement around the H^+ was actually predicted from the calculations. One would expect this angle to be even closer to 180° with *t*-BuLi as a base. The angles around the leaving H^+ are 165° and 175° for α- and β-lithiation transition structures, as compared with 174° for the transition structure for CH_3Li and CH_4. The optimized geometries of the reactant complexes and transition structures are shown in Figure 10.

Based on generalizations from the previous calculations with LiH, it seems reasonable that the essential geometrical features for β'-lithiation and cis- and trans-γ-lithiation with CH_3Li as a base would be unchanged vis-à-vis β-lithiation with CH_3Li as a base. The "ideal" C–H–C attack angle should be 165–175°, and the Li–CH_3–H angle around 45–55°. The H–C–Li angle, the angle around the developing carbanion, should also be 45–55°. Both the forming H–CH_3 and the breaking H–C^- bond lengths should be 1.45–1.50 Å, while the distance between the developing carbanion center and lithium should be 2.1–2.3 Å, which is close to the lithium–base distance in the transition structure. Finally, a favorable Li–N coordination involved in the transition structure requires the distance to be 1.9–2.0 Å.

In summary, our calculations are in good agreement with the experimental observations that cis-γ-lithiation and β-lithiation are both preferred over α-lithiation and β'-lithiation. Trans-γ-lithiation is least favored. The transition state for lithiation appears to be very product-like (late transition state) with the new C–Li bond substantially formed at the transition state. ^{13}C NMR experiments with chelating and nonchelating enamine complexes with *n*-BuLi show that the two complexes are qualitatively different. The presence of the second amino group allows for better coordination (chelation effect) to the otherwise weak enamine moiety, thus facilitating lithiation. Additional donor molecules or binding sites on the chelating group may saturate the electrophilic *t*-BuLi, inhibiting binding to the relatively weak enamine nitrogen, thus inhibiting metalation. The chelating group may play an additional role in stabilizing the resulting lithiated species by preventing the solvent reorganization necessary for rearrangement to more resonance stabilized carbanions.

Acknowledgment. We are grateful to the National Institutes of Health and the National Science Foundation for the financial support of this research.

Registry No. $CH_2{=}CHNH_2$, 593-67-9; $CH_2{=}C(CH_3)NH_2$, 4427-28-5; $CH_3CH{=}CHNH_2$, 43691-07-2.

(28) Rondan, N. G.; Houk, K. N., unpublished results.

(29) **Note Added in Proof**: After prolonged refluxing, lithio-**2a** did not exchange a proton with **2b**, nor did lithio-**2b** exchange a proton with **2a**, as determined by deuterium quenching experiments.

Computational Studies of the Interactions of Chiral Molecules: Complexes of Methyl *N*-(2-Naphthyl)alaninate with *N*-(3,5-Dinitrobenzoyl)leucine *n*-Propylamide as a Model for Chiral Stationary-Phase Interactions

Sid Topiol,* Michael Sabio, June Moroz, and Walton B. Caldwell

Contribution from the Department of Medicinal Chemistry, Berlex Laboratories, Inc., 110 East Hanover Avenue, Cedar Knolls, New Jersey 07927. *Received March 28, 1988*

Abstract: The complexes of (*S*)-methyl *N*-(2-naphthyl)alaninate (NAP) with both enantiomers of *N*-(3,5-dinitrobenzoyl)leucine *n*-propylamide (DNB) were studied as models for the interactions responsible for the separation of enantiomers with the chiral stationary phase systems developed by Pirkle and co-workers. The interaction model investigated is that presented by Pirkle et al. On the basis of molecular mechanics and semiempirical and ab initio quantum mechanical calculations it is suggested that (i) all of the primary components of the interactions of the two complexes are identical in nature and similar in magnitude and (ii) the π–π interactions between the dinitrobenzoyl and naphthyl groups are not the primary components of the complex stabilization and enantiomer separation. Enantiomer differentiation, in this model, could only be achieved via small through-space field effects and not through a classical three-point attachment mechanism. Alternatively, chiral separation is achieved through other mechanisms.

There has been an increasing interest in the separation of enantiomeric compounds by various methods. Theoretical models for the interactions of chiral molecules are often subtle and quite challenging. Indeed, a number of new models have recently been described.[1-4] Of perhaps more practical interest is the increasing awareness of the importance of separating enantiomers. This is particularly true in medicinal chemistry where many drugs often

(1) Topiol, S. A General Criterion for Molecular Recognition: Implications for Chiral Interactions. *Chirality*, in press.

0002-7863/88/1510-8367$01.50/0 © 1988 American Chemical Society

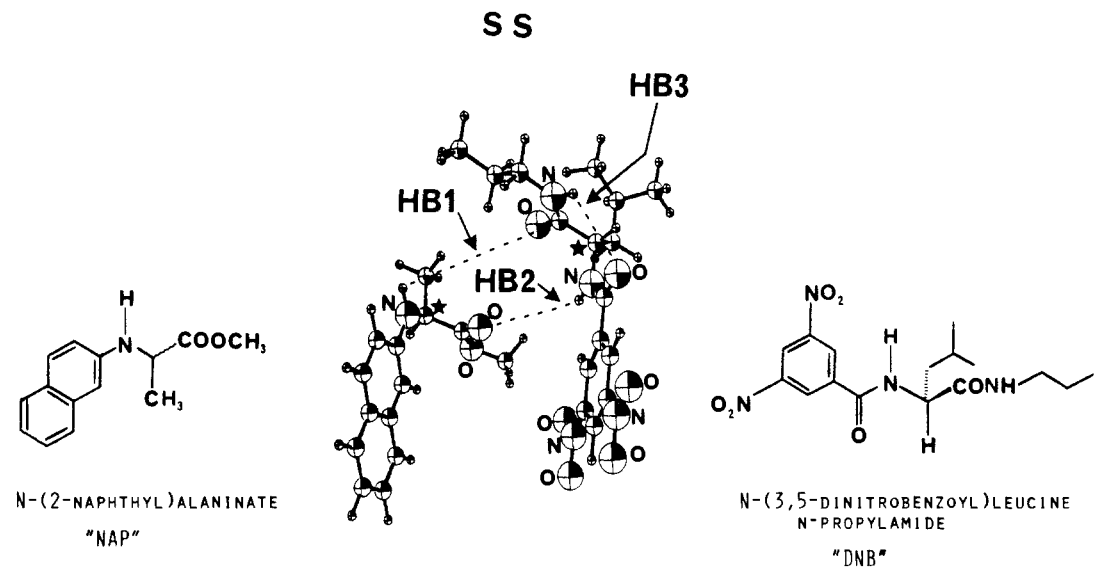

Figure 1. Schematic representation of the interaction model for *S*-NAP with *S*-DNB. HB1 and HB2 represent the two hydrogen bonds. FF or "front/front" defines the relative orientation of the naphthyl ring to the dinitrobenzoyl ring as shown.

contain chirotopic centers. As has been recently emphasized,[5] the biological activities of two enantiomers can be quite different. Thus, while one enantiomer of a chiral compound may be active on some receptor system, its enantiomer may be inactive, of equal activity, synergistic (positively or negatively), or antagonistic on the same receptor system. Indeed, the other enantiomer may have an entirely different profile of activities on other receptor systems, possibly even including toxic effects.[5] These differences in activities reflect differences in the molecular mechanisms of ligand/receptor interactions for the two enantiomers. Advances in the understanding of the different interactions of the enantiomers of chiral molecules therefore represent an important area in drug research.

Because of these different possible mechanisms for drug action of chiral molecules, it is often necessary to separate enantiomers. While it is sometimes possible to accomplish this during synthesis, typically both enantiomers are synthesized in significant amounts and must be separated afterwards. A number of different separation methods are currently being developed.[6-11] We present herein computational studies on models of the chiral stationary phase (CSP) systems developed by Pirkle and co-workers.[11-13] In these systems, one enantiomer of *N*-(2-naphthyl)amino acids is attached to a silica gel stationary column and used to separate enantiomers of *N*-(3,5-dinitrobenzoyl)amino acids. Similarly, these workers have also developed the "reciprocally" related CSPs, by using columns made by anchoring *N*-(3,5-dinitrobenzoyl)amino acids to a stationary column to separate enantiomers of *N*-(2-naphthyl)amino acids. The goal of the present study is to gain a better understanding of the molecular mechanism by which these CSPs work as well as to gain insights into the differences of the interactions of enantiomers with biological receptors. Toward this end, Lipkowitz and co-workers have already reported conformational studies on models of these analytes and chiral stationary phases as isolated fragments.[14-17] Also, interaction models of complexes for related systems have been studied with use of rigid and relaxed structures of the fragments.[18-20,31]

Methods

Completely relaxed geometries of the complexes of (*S*)-methyl *N*-(2-naphthyl)alaninate with the *R* and *S* enantiomers of *N*-(3,5-dinitrobenzoyl)leucine *n*-propylamide were obtained by using the molecular mechanics MMFF program within CHEMLAB-II (Revision 9.0).[21] Substructures derived from the fully optimized complexes were generated in CHEM-X[22] in order to model the important interactions in the complexes. By using the semiempirical quantum chemical AM1[23] method as implemented in AMPAC (Version 1.00),[24] energies of interaction were calculated for the MMFF completely relaxed geometries of the complexes (and frozen fragments thereof) and for local minima found in QXQ[25] scans with AM1 derived point charges. Ab initio Hartree–Fock[26] calculations using the STO-3G[27] basis set were performed with the GAUSSIAN 80[28] system of programs to investigate the nature of the interactions in the complexes via the Morokuma energy decomposition scheme.[29]

(2) Boehm, R. E.; Martire, D.; Armstrong, D. W. *Anal. Chem.* **1988**, *60*, 522.
(3) Lipkowitz, K. B.; Zegarra, R. Theoretical Studies in Molecular Recognition: Rebek's Cleft. *J. Comput. Chem.*, in press.
(4) Salem, L.; Chupaisat, X.; Segal, G.; Hiberty, P. C.; Minot, C.; Loferestier, C.; Sautet, P. *J. Am. Chem. Soc.* **1987**, *109*, 2887.
(5) Ariens, E. J. *Trends Pharmacol. Sci.* **1986**, *7*, 200, and references therein.
(6) Armstrong, D. W. *Anal. Chem.* **1987**, *59*, 84A.
(7) Armstrong, D. W. *J. Liq. Chromatogr.* **1987**, *7*(*S-2*), 353.
(8) Okamoto, Y. *Chemtech* **1987**, *17*, 176.
(9) Allenmark, S. *J. Biochem. Biophys. Meth.* **1984**, *9*, 1.
(10) Davankov, V. A.; Kurganov, A. R.; Bochkov, A. S. *Adv. Chrom.* **1984**, *22*, 71.
(11) Pirkle, W. H.; Finn, J. In *Asymmetric Synthesis*; Morrison, J. D., Ed.; Academic Press: New York, 1983.
(12) (a) Pirkle, W. H.; Pochapsky, T. C. *J. Am. Chem. Soc.* **1987**, *109*, 5975. (b) Pirkle, W. H.; Pochapsky, T. C. *Ibid.* **1986**, *108*, 5627.
(13) Pirkle, W. H.; Pochapsky, T. C. *J. Am. Chem. Soc.* **1986**, *108*, 352.
(14) Lipkowitz, K. B.; Demeter, D. A.; Landwer, J. M.; Parish, C. A.; Darden, T. *J. Comput. Chem.* **1988**, *9*, 63.
(15) Lipkowitz, K. B.; Demeter, D. A.; Parish, C. A.; Landwer, J. M.; Darden, T. *J. Comput. Chem.* **1987**, *6*, 753.
(16) Lipkowitz, K. B.; Landwer, J. M.; Darden, T. *Anal. Chem.* **1986**, *58*, 1611.
(17) Lipkowitz, K. B.; Malik, D. J.; Darden, T. *Tetrahedron Lett.* **1986**, *27*, 1759.
(18) Lipkowitz, K. B.; Demeter, D. A.; Parish, C. A. *Anal. Chem.* **1987**, *59*, 1731.
(19) Still, M. G.; Rogers, L. B., unpublished results.
(20) Norinder, U.; Sundholm, E. G. *J. Liq. Chromatogr.* **1987**, *10*, 2825.
(21) CHEMLAB-II, Molecular Design Ltd., San Leandro, CA.
(22) CHEM-X, developed and distributed by Chemical Design Ltd., Oxford, England.
(23) Dewar, M. J. S.; Zoebisch, E. G.; Healy, E. F.; Stewart, J. J. *J. Am. Chem. Soc.* **1985**, *107*, 3902.
(24) Dewar Research Group; Stewart, J. J. P. AMPAC, version 1.00, Quantum Chemistry Program Exchange, program no. 506, 1986.
(25) Osman, R.; Rubenstein, L. QXQ (private communication).
(26) Roothaan, C. C. J. *Rev. Mod. Phys.* **1960**, *32*, 179.
(27) Hehre, W. J.; Stewart, R. F.; Pople, J. A. *J. Chem. Phys.* **1969**, *51*, 2657.
(28) Binkley, J. S.; Whiteside, R. A.; Krishnan, R.; Seeger, R.; DeFrees, D. J.; Schlegel, H. B.; Topiol, S.; Kahn, L. R.; Pople, J. A. Department of Chemistry, Carnegie-Mellon University, Pittsburgh, PA 15213, 1980.
(29) Morokuma, K. J. *J. Chem. Phys.* **1968**, *55*, 1236.

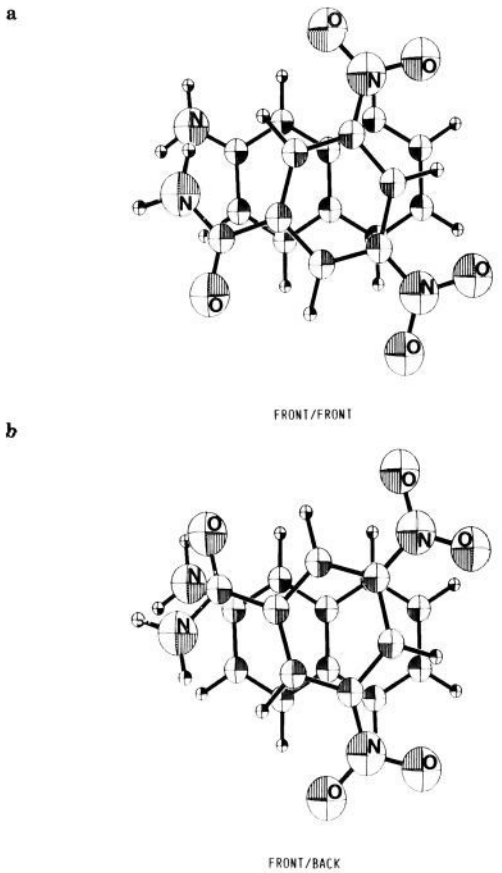

Figure 2. Structures used to model the $\pi-\pi$ interaction complexes: (a) front/front and (b) front/back.

Results

The Interaction Model Studied. In the present study, the *S* enantiomer of methyl *N*-(2-naphthyl)alaninate (NAP, **1**) is used as the model for the stationary phase resolving agent, and the two enantiomers of *N*-(3,5-dinitrobenzoyl)leucine *n*-propylamide (DNB, **2**) serve as the model compounds of the mobile phase which would be separated by the former (Figure 1). In the usual experimental arrangement, **1** would be attached to the stationary phase silica gel through the methoxy methyl group.[13] In the design of these systems, the naphthyl group of **1** and the dinitrobenzoyl group of **2** have been incorporated so as to generate a π-donor–acceptor stacking interaction between these two regions in the formation of the complex. In addition, two intermolecular hydrogen bonds have been proposed[12] as indicated in Figure 1. These three interactions are considered responsible for chiral resolution by means of a classical three-point interaction model.[30] Specifically, only one enantiomer (*S*) of **2** is expected to be capable of undergoing all three stabilizing interactions simultaneously with the *S* enantiomer of **1**.[12] As will be discussed below, we find that both complexes can achieve these same primary interactions, and therefore this scheme does not explain chiral separation for these systems.

Figure 1 then schematically represents the interaction model for the *S* isomers of **1** and **2** (hereafter referred to as SS, analogous notation used for other complexes) proposed by Pirkle and coworkers and as supported by their spectroscopic studies.[12] We note that there is also the possibility for an intramolecular hydrogen bond in **2** between the *n*-propylamide and the benzoyl oxygen atom (Figure 1). Our calculations presented below support this possibility.

Other possible schemes for the intermolecular complexes were found in our preliminary calculations and studies of other investigators.[31] The energetic analysis of these other possible modes of interaction, together with those studied here, and any other possibilities, could be used in the construction of a statistical mechanical analysis to predict chiral separation. Two such schemes have recently been proposed by Boehm et al.[2] and Lipkowitz et al.[3] The present work is however limited to an analysis of the model described.

Relative Orientation of the π Complex. The relative orientation assumed for the two planar portions of the complex is herein referred to as front–front or FF (and analogous notations for the other relative orientations; Figure 2). This corresponds to the orientation found by Pirkle and Pochapsky[12] for these compounds in solution based on NOE studies. The planar regions above can be modeled by the complexes shown in Figure 2. The front–back interaction is not equivalent to the front–front interaction. Thus, a scan of the interaction energies using point-charge representa-

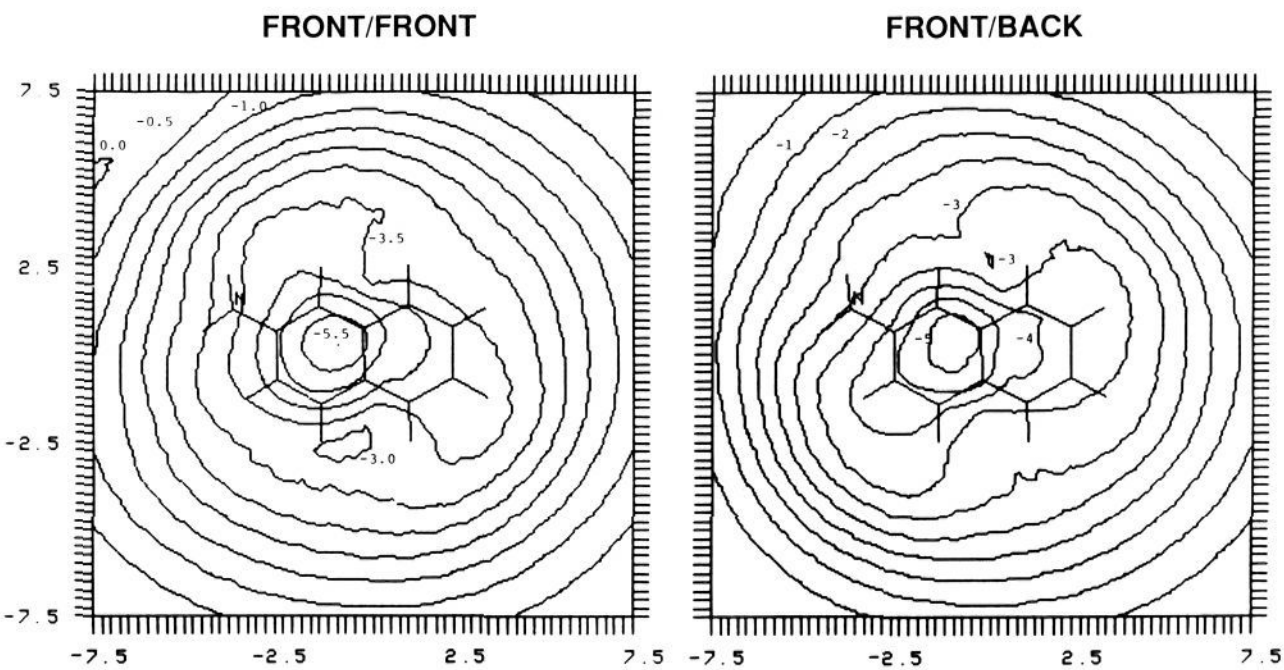

Figure 3. Maps of the electrostatic interaction energy scans for the $\pi-\pi$ interaction model PPI in a front/front and front/back relative orientation (see Methods section for details).

Table I. NAP(PPI)/DNB(PPI) Interaction Energies (in kcal/mol) at the Local Minima

	electrostatic interaction energies using AM1 charges		AM1 interaction energies	
	total	relative	total	relative
		"Front/Front"		
A	−5.50	0.0	8.71	6.77
B1	−3.08	2.42	3.78	1.76
B2	−3.07	2.43	3.84	1.90
B3	−3.08	2.42	4.27	2.33
B4	−3.13	2.37	4.27	2.33
C1	−3.57	1.93	1.94	0.0
C2	−3.51	1.99	2.06	0.12
D1	−3.73	1.77	4.60	2.67
D2	−3.73	1.77	5.63	3.69
		"Front/Back"		
A	−5.26	0.0	8.88	4.02
B	−3.03	2.22	4.86	0.0

tions of both portions, keeping the two systems parallel with a 3.0-Å separation and moving the dinitrobenzoyl portion with respect to a fixed naphthyl portion, gives different results for the FF and FB complexes (Figure 3). While the two electrostatic interaction energy maps shown in Figure 3 are different, both show a tendency for the dinitrobenzoyl to stay somewhat localized over the naphthyl ring. Figure 4 shows the various local minima found for these two complexes. There are nine local minima found for the FF complex and two for the FB. The nine local minima of the FF scan have been arbitrarily grouped into four clusters based on similar geometries. Cluster A (one structure) has a maximal overlap which is significantly greater than that of the other three clusters. Cluster C has the least overlap. For the FB interaction, there are two structures and the one with maximal overlap is labeled A. The total and relative electrostatic interaction energies for these complexes are shown in Table I. These interaction energies are all stabilizing. The most stable in each set (FF or FB) is the structure with maximal overlap (i.e., A in both cases).

These results are quite different when the interaction energy is calculated with use of the semiempirical quantum chemical AM1 method with the same structures. All of the interaction energies are repulsive in the AM1 calculations. At the AM1 level, the structures with greatest overlap have the highest energy. The implications of this for the systems studied here will be discussed further below.

As the full complexes are not planar, the FF, FB, BF, and BB relative orientations of the SS and SR complexes should all be considered, i.e., a total of eight possibilities. For the present study we will focus on the FF relative orientation for the π region as this corresponds to that found in the experimental work of Pirkle and Pochapsky.[12] Also, while the above comparison shows qualitative differences between the results with different methods of calculation, the FF and FB interactions seem similar in nature. The other possibilities are presently under investigation and will thus be reported elsewhere.

Molecular Electrostatic Potentials. The separation of the *R* and *S* enantiomers of DNB results from the difference in binding energy to *S*-NAP. This suggests a difference in recognition elements for *R*- and *S*-DNB. Such recognition elements are long range effects. As indicators of these long range effects, the molecular electrostatic potentials (MEPs) of *R*- and *S*-DNB in four different planes have therefore been evaluated with AM1 derived point charges (Figures 5–8). As enantiomer separation must be a result of the differences in recognition elements between *R*- and *S*-DNB, we show the MEPs of both in each figure. The structure of *R*-DNB was taken from the optimized structure of the SR complex in a molecular mechanics calculation by using the MMFF procedure; for the MEPs of *S*-DNB, the structure of *S*-DNB was derived from the optimized structure of *R*-DNB by interchange of the proton and *sec*-butyl group. We note that it may seem inconsistent to use this structure for *S*-DNB obtained in this way rather than from the SS complex. However, we are examining the MEPs as recognition criteria of the isolated enantiomers. If we had taken the structure of *R*-DNB from the SR complex and *S*-DNB from the SS complex, then differences in the MEPs would reflect not only differences of the isolated enantiomers but also differences of the diasteriomeric complexes.

Figures 5 and 6 highlight recognition elements based on the π interactions. Figure 5 shows the MEPs of *R*- and *S*-DNB in the plane of the naphthyl portion of NAP (i.e., approximately 3.0 Å from the dinitrobenzoyl ring). Figure 6 shows the MEP in a plane 1.5 Å closer to *R*- and *S*-DNB. Thus, Figure 5 represents what the nuclear framework of the naphthyl ring "sees" due to DNB, while Figure 6 represents what the π cloud of the naphthyl ring senses. In both sets of maps, there is very little difference between *R*- and *S*-DNB. This would suggest that the π- interaction alone is not responsible for enantiomer separation.

Figures 7 and 8 are focused on the oxygen atom of the propylamide of *R*- and *S*-DNB. This is the oxygen atom which would act as a proton acceptor for the amine hydrogen atom of NAP in one of the two suggested hydrogen bonds (HB1). The maps shown in Figure 7 are taken in a plane perpendicular to the C=O bond at a distance of 1.5 Å from the oxygen atom, while the maps in Figure 8 are taken in the plane containing the C=O bond and perpendicular to the amide group. Here too, the MEPs of *R*- and *S*-DNB are very similar in both cases. Thus, the MEPs of the *R* and *S* enantiomers of DNB provide no obvious explanation for enantiomer separation.

Interaction Energy Analysis. As the analysis of the MEPs above did not provide an explanation for enantiomer separation, we evaluated the interaction energies of *S*-NAP with *R*- and *S*-DNB. Complete structural optimizations, including all geometrical parameters, were performed for both the SS and SR complexes (only in the FF relative orientations of the π regions) with the molecular mechanics MMFF method. The optimized structures are shown in Figure 9. As indicated in Figure 9, all three interactions (π and two hydrogen bonds) as well as the intramolecular hydrogen bond in DNB are present for both complexes.

In order to more rigorously analyze the interactions in these complexes, model systems were constructed as shown in Figure 10. The complexes PPI and PPI-SM were designed to model the π interactions. Similarly, the HB1 and HB2 complexes were designed to model the two hydrogen bonds. As a test of how well these three models represent the complete interaction of the complex, AM1 calculations were done for the full complexes and the models with use of the structures obtained from the molecular mechanics calculations described above. The results are presented in Table II.

For both the SS and SR complexes the sum of the interactions for the three model structures PHB1, PHB2, and PPI (−4.53 kcal/mol and −4.19 kcal/mol, respectively) is very nearly equal to that of the full complex (−5.19 kcal/mol and −4.96 kcal/mol, respectively). In addition, the PPI-SM interaction energies are very similar to the PPI interaction energies in the AM1 calculations. This supports the use of the models described here.

At the AM1 level both complexes are stable. The total energy of the SS complex is 0.89 kcal/mol lower than that of the SR complex. The difference in the stabilization energies of the SS and SR complexes relative to the corresponding frozen isolated compounds is 0.23 kcal/mol. Thus, these computational results are in agreement with experiment (however, see below). In both sets of model complexes, the two hydrogen bonds are stable. HB2 is more stable than HB1, which is consistent with the NOE results of Pirkle and Pochapsky.[12] Surprisingly, as discussed earlier (e.g., Table I) the PPI and PPI-SM models have repulsive interaction energies. As discussed below, this is probably an artifact of the use of the structures obtained from the MMFF calculations.[35,37,38] Note that the structures of the full complexes do indicate that these portions are in positions appropriate for π-type interactions.

The ab initio results using the STO-3G basis set are very similar to those of the AM1 calculations. The sum of the interaction energies of the models are similar in magnitude (−5.16 and −4.64 kcal/mol for the SS and SR structures, respectively). The dif-

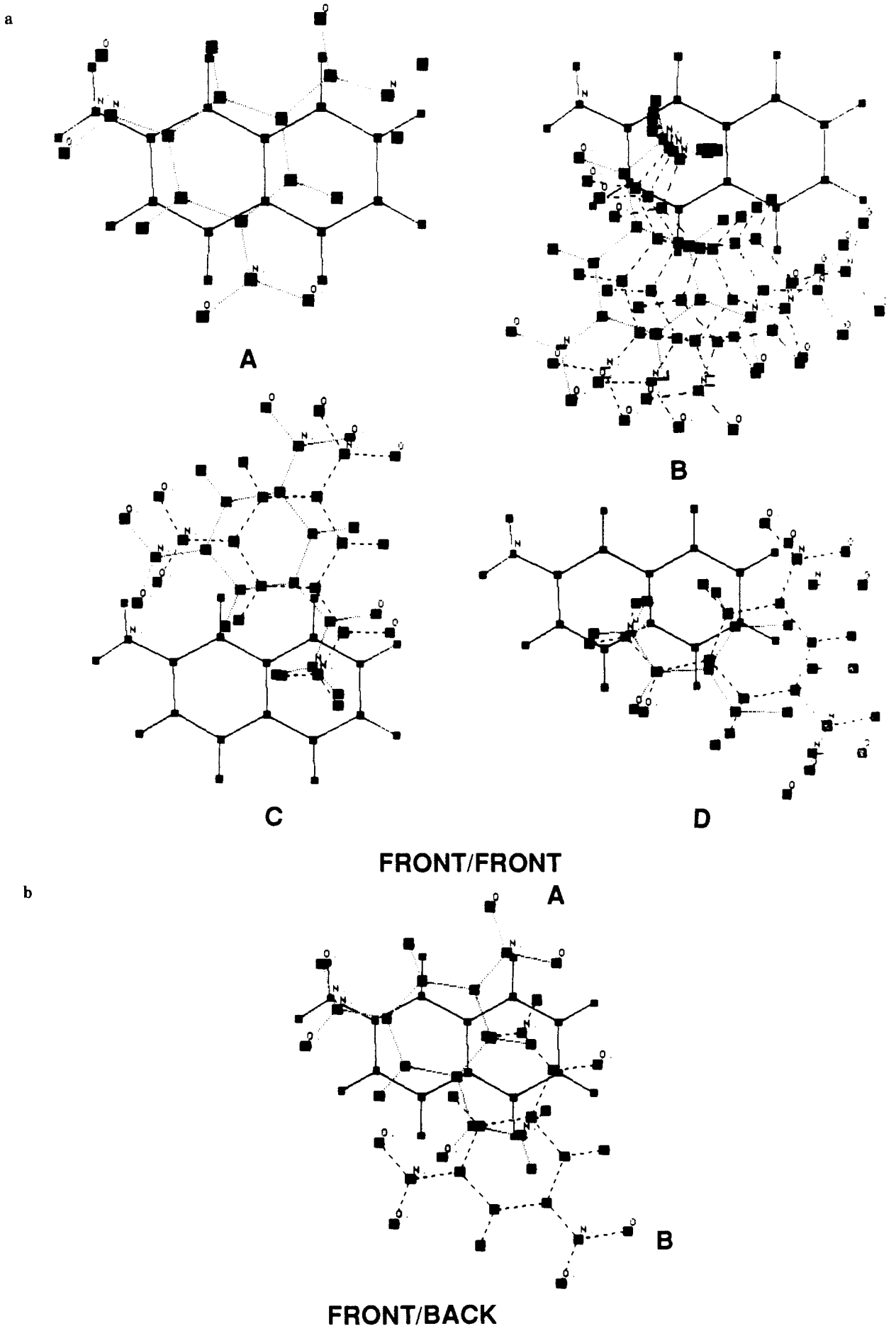

Figure 4. Local minima of the electrostatic interaction energy scans for the $\pi-\pi$ interaction model in Figure 3: (a) the nine local minima for the front/front scan and (b) the two local minima for the front/back scan.

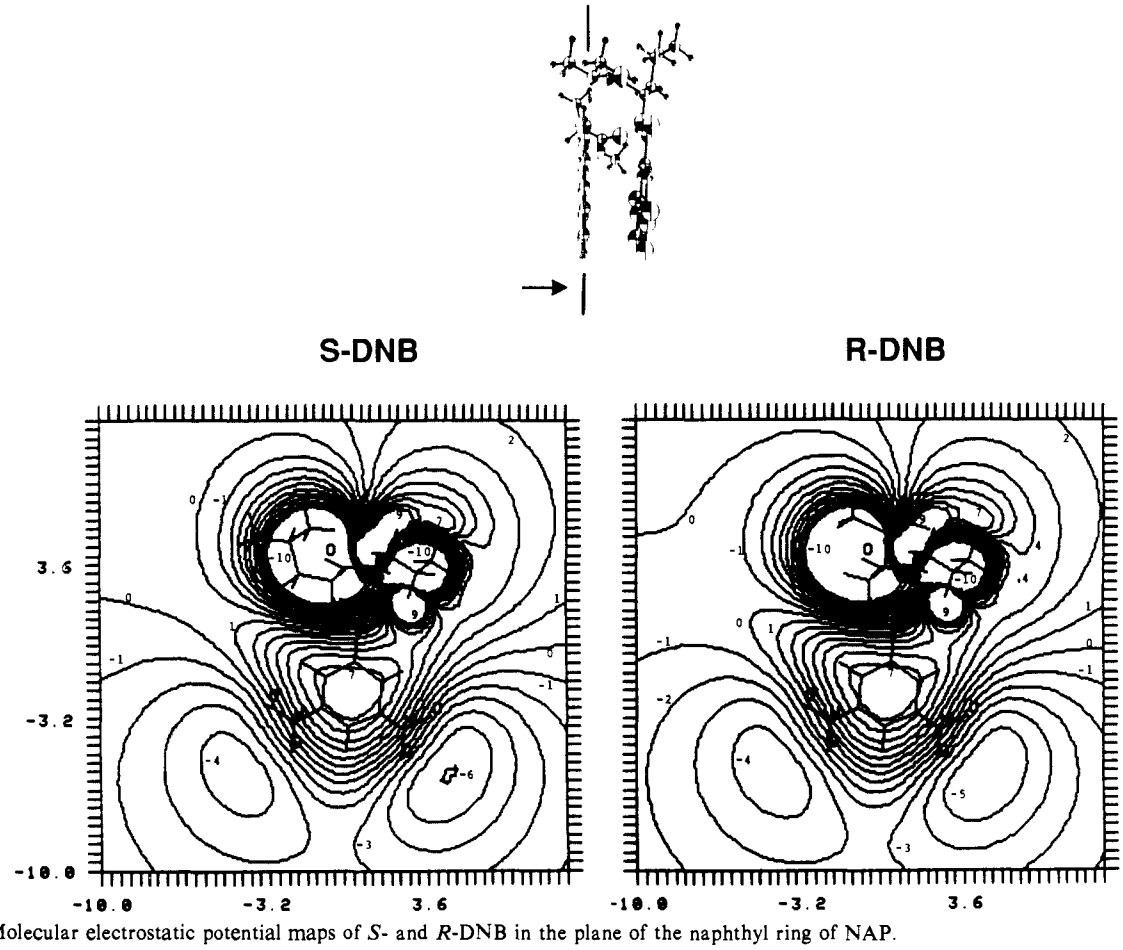

Figure 5. Molecular electrostatic potential maps of *S*- and *R*-DNB in the plane of the naphthyl ring of NAP.

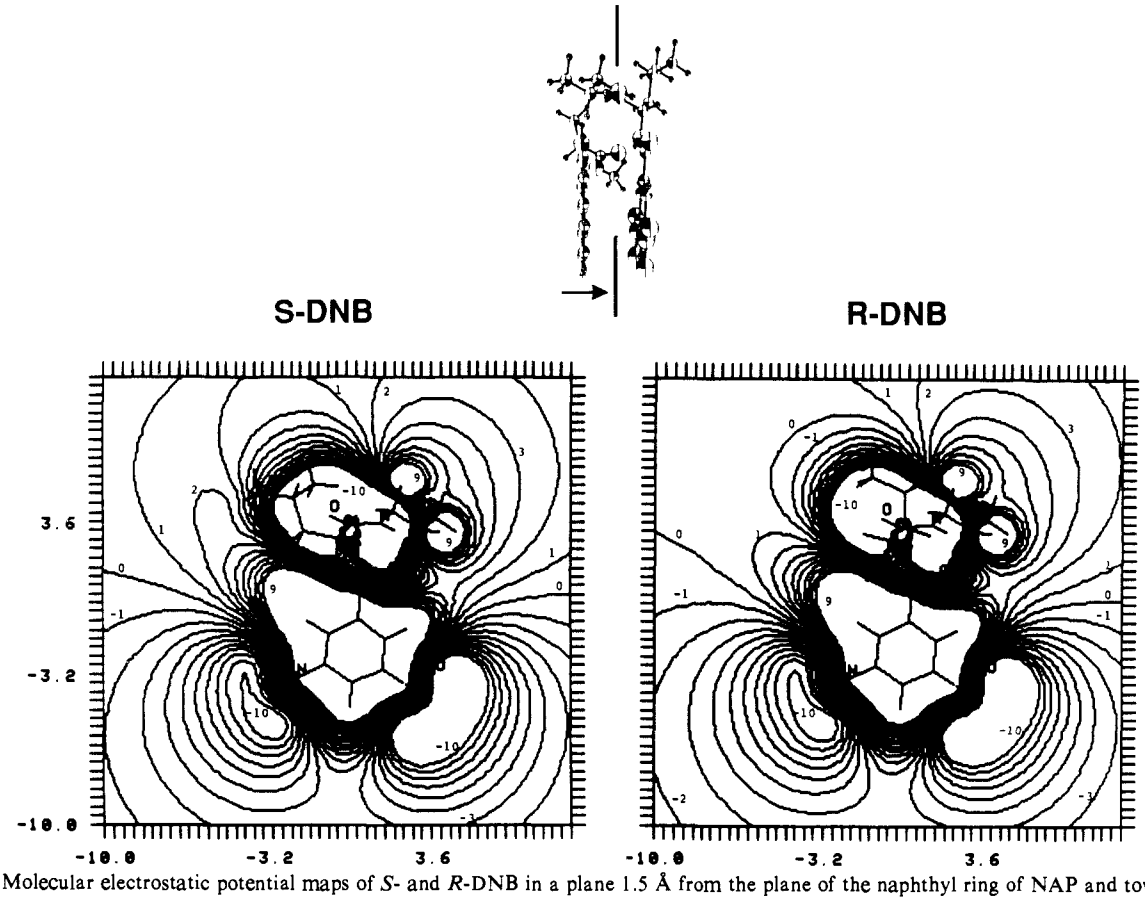

Figure 6. Molecular electrostatic potential maps of *S*- and *R*-DNB in a plane 1.5 Å from the plane of the naphthyl ring of NAP and toward DNB.

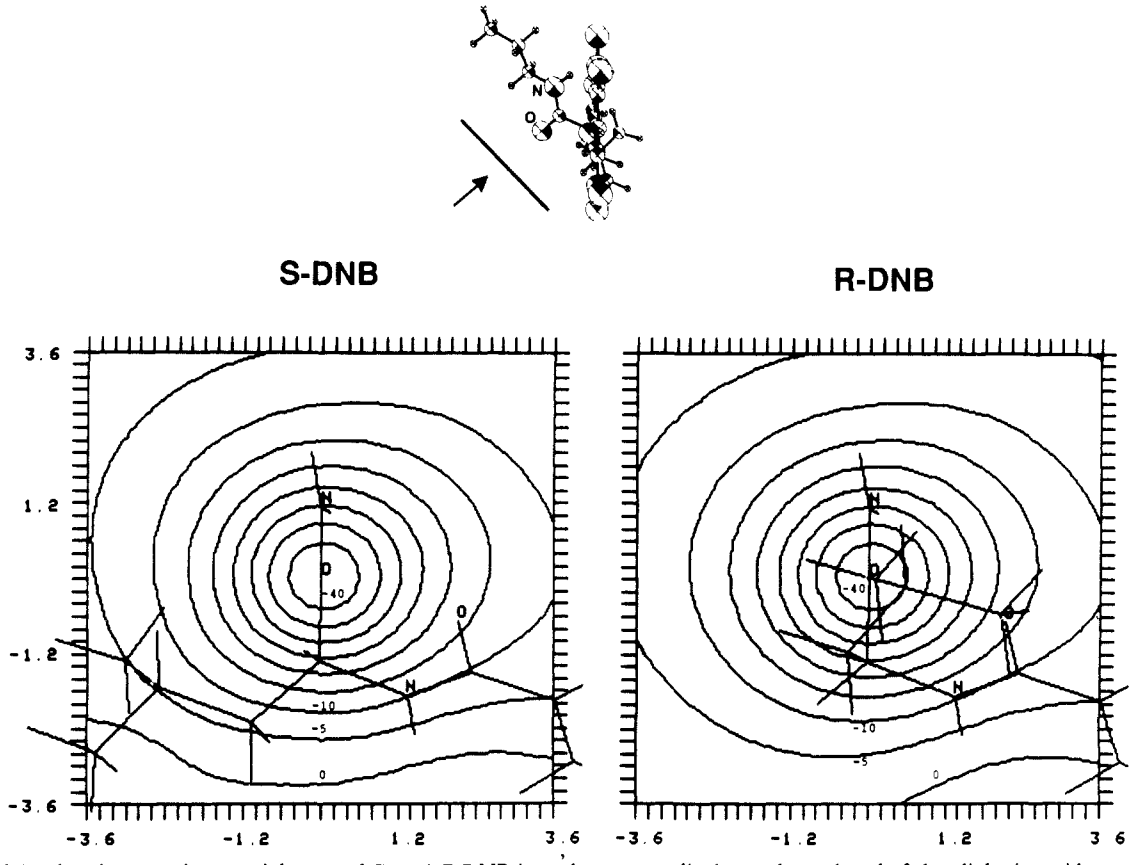

Figure 7. Molecular electrostatic potential maps of *S*- and *R*-DNB in a plane perpendicular to the carbonyl of the aliphatic amide.

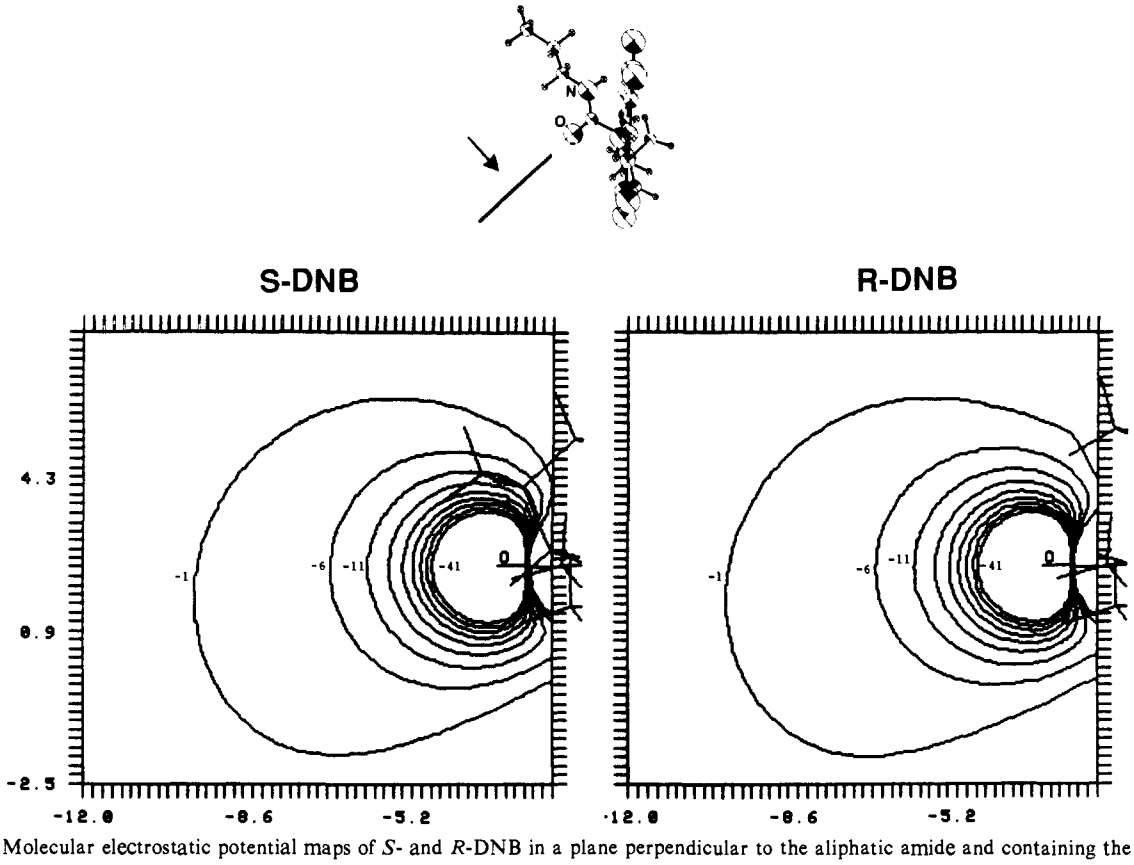

Figure 8. Molecular electrostatic potential maps of *S*- and *R*-DNB in a plane perpendicular to the aliphatic amide and containing the C=O bond.

ference between the sums of the PHB1, PHB2, and PPI-SM interaction energies at the STO-3G level (0.52 kcal/mol) is only 0.30 kcal/mol different from that at the AM1 level (0.22 kcal/mol). Again there is a slight preference for the SS complex. The PPI-SM interaction is again repulsive at the STO-3G level for both complexes (probably for the same reasons).[35,37,38] Further analyses of these interactions were done with the Morokuma energy decomposition scheme.[29] These results (Table II) show that the both PHB1 and PHB2 are predominantly electrostatic in nature for the SS and SR structures as would be expected for

Table II. Interaction Energies (in kcal/mol) of Model Fragments

AM1									
PHB1		PHB2		PPI-SM		PPI		FULL	
SS	SR	SS	SR	SS	SR	SS	SR	SS	SR
−2.94	−2.91	−5.20	−4.97	3.70	3.66	3.61	3.69	−5.19	−4.96

Sum (PHB1 + PHB2 + PPI-SM) = −4.44 (SS); −4.22 (SR)
Sum (PHB1 + PHB2 + PPI) = −4.53 (SS); −4.19 (SR)

Morokuma Energy Decomposition Analysis (STO-3G Basis Set)

	PHB1		PHB2		PPI-SM	
	SS	SR	SS	SR	SS	SR
electrostatic	−2.31	−2.27	−3.29	−3.02	−1.42	−1.44
polarization	−0.16	−0.16	−0.25	−0.29	−0.13	−0.13
charge transfer[a]						
N to D	−0.10	−0.09	−1.59	−1.56	−0.56	−0.56
D to N	−1.99	−1.97	−0.27	−0.24	−0.21	−0.20
exchange	2.17	2.15	1.42	1.45	3.40	3.45
mixing	0.04	0.04	0.03	0.03	0.08	0.08
total	−2.35	−2.30	−3.96	−3.54	1.15	1.20

Sum (PHB1 + PHB2 + PPI-SM) = −5.16 (SS); −4.64 (SR)

[a] N and D refer to the naphthyl and dinitrobenzoyl models, respectively.

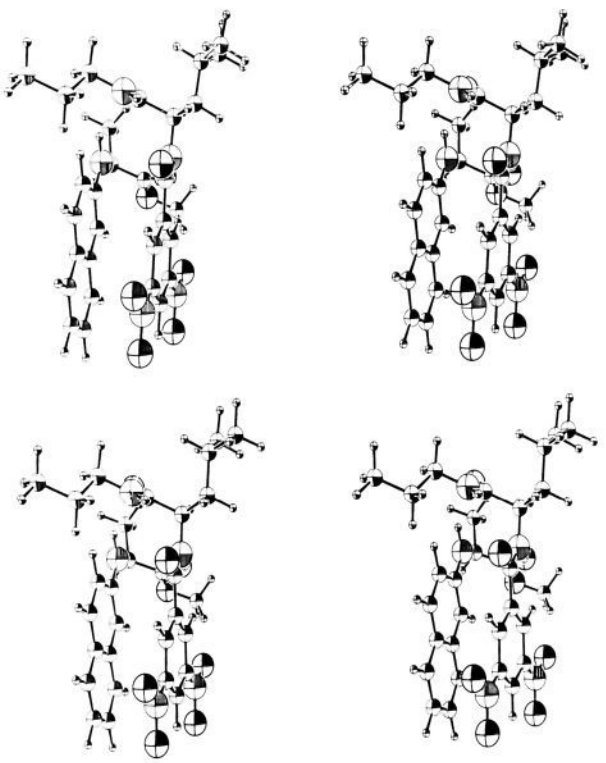

Figure 9. Stereo drawings of MMFF optimized structures of the SSFF (upper structure) and SRFF (lower structure) complexes of *S*-NAP with *S*- and *R*-DNB.

hydrogen-bonding systems. On the other hand, the PPI-SM models are dominated not by the charge-transfer terms as would be expected but rather by the exchange repulsion terms; this too probably relates to the use of the MMFF structures. As expected, the contribution of charge from the naphthyl to dinitrobenzoyl portions contributes more to the stabilizing effects of this component of the interaction energy than does charge transfer from the dinitrobenzoyl to the naphthyl portion.

Discussion

An important consideration in evaluating the results of these studies is that the energy differences between the SS and SR complexes for the various models presented here by the different computational methods are quite small, i.e., less than 1.0 kcal/mol. Certainly, none of the methods used herein can predict the values of the total interaction energies to such a high accuracy. Thus, the fact that, consistent with experimental results, the small energy differences consistently favor the SS complex over the SR may indeed be fortuitous. It is, however, possible that even if the values of the interaction energies are in error by much larger amounts, the interaction energy *differences* may be reliable. This is because the two complexes are so similar that one could expect a significant cancellation of errors. It would therefore be interesting to conduct a careful calibrative study to see if this can be verified. For the present analysis, as will be seen below, it is sufficient to have established that the energy differences between the SS and SR complexes are small, i.e., less than 1 kcal/mol.

Perhaps the most important finding of the present work is the similarity of the SR complex (in structure and interaction energies) to the model proposed for the SS complex.[12] As Lipkowitz has pointed out,[14] while a model for the SS complex has been proposed by Pirkle and co-workers[12] (and supported by NOE results), this did not provide an explanation for chiral recognition. Rather, an analysis of a model for the SR complex is also required. The model for the SS complex proposed by Pirkle et al. is used as the basis for chiral recognition through a classical three-point model: "One can see that by interchanging any two groups on either stereogenic center, at least one of the attractive interactions shown for the (*S*)-**1b**–(*S*)-**2b** complex will be lost"[12a] (where (*S*)-**1b**–(*S*)-**2b** is equivalent to the SS complex herein). In contrast to this, we have shown that the same three primary interactions (attractive or repulsive) are in fact possible for both complexes (see Figure 9). To state if differently, the model proposed for the SS complex cannot be the basis for chiral resolution via a classical three-point model. This may be more easily appreciated with the aid of Figure 11. Figure 11a depicts the classical three-point model for chiral resolution. In that model, only one enantiomer can simultaneously form the three critical interactions (aa′, bb′, and cc′). The three interactions in that model lie along three different bonds emanating from the chiral center.[32,33] Figure 11b shows a schematic representation of the three interactions in the present complex. The three primary interactions (aa′, bb′, and cc′ in Figure 11b or the two intermolecular hydrogen bonds and the π interaction in Figure 9) occur with functional groups which lie along only two of the bonds of the chirotopic center. Alternatively, one can consider starting with the model for the SS complex (or Figure 11b upper structure) and converting it to the SR complex (Figure 11b lower structure) by interchanging the hydrogen and *sec*-butyl groups (d′ and f′ in Figure 11b). This can be achieved without losing one of the "points-of-attachment". Thus, if the structure of the SS complex is correctly described by the model, then the SR complex need not differ in the primary interaction but rather in the through-space field effects resulting from the interchange of

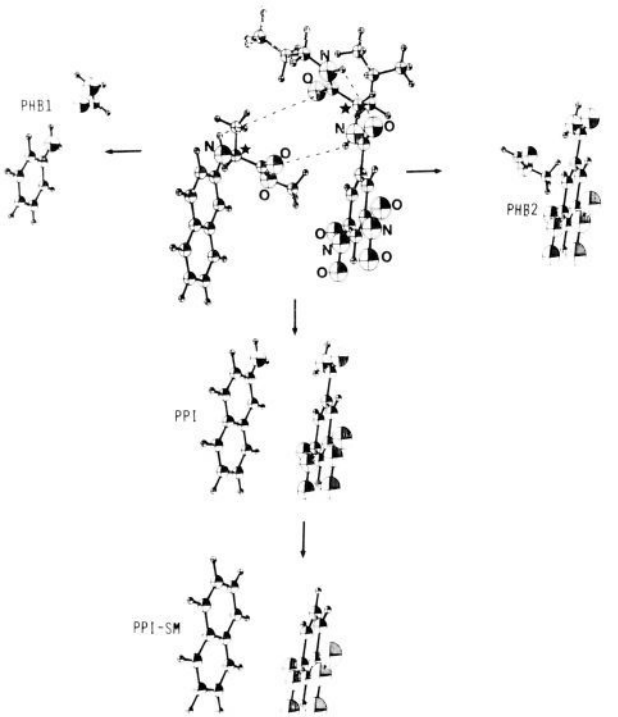

Figure 10. Schematic representation of the model fragments of the NAP/DNB complex.

the hydrogen and the *sec*-butyl groups. These groups are situated outside of the region of the primary interaction and would be expected to have very small effects on the differences of the interaction energies.

These results are in fact consistent with experiment. Typical separability factors for chiral stationary phase experiments using these systems are on the order of 1.0–1.5, suggesting differences in the free energies of interaction of ca. 0.5 kcal/mol or less. On the other hand, loss of a primary interaction such as a hydrogen bond (i.e., a genuine three-point mechanism) would give free energy differences on the order of 2–4 kcal/mol. This would then lead to separability factors of 100–200. Thus, while a three-point model is unlikely to be operative in this system (or indeed in most chiral stationary phases, based on this energetic analysis), it can still serve as a guide in the design of more efficient CSPs. In addition to the agreement between the structures found here for the SS complex with the experimental model[12] we note that these structures are also consistent with the conformations obtained with force field calculations of the isolated NAP and DNB systems.[14-17]

The small preference of the total and components of the interaction energy differences for the SS complex versus those of the SR complex are thus qualitatively and quantitatively consistent with experiment, albeit possibly fortuitously. Nevertheless, it is somewhat unexpected to find that not only are all the local minima of the PPI model repulsive in the AM1 calculations (Table II), but even the ab initio STO-3G calculations predict the π interaction to be repulsive. It thus appears that the two hydrogen bonds drive the complex into a conformation which forces the π interaction. In this regard we make three observations.

Firstly, this is consistent with the experimental structure activity studies of Wainer et al.: "These results suggest that the $\pi-\pi$ interactions between an aromatic substituent on the amide moiety of the solute and the dinitrobenzoyl substituent of the CSP apparently have a limited stabilizing effect on the diastereomeric

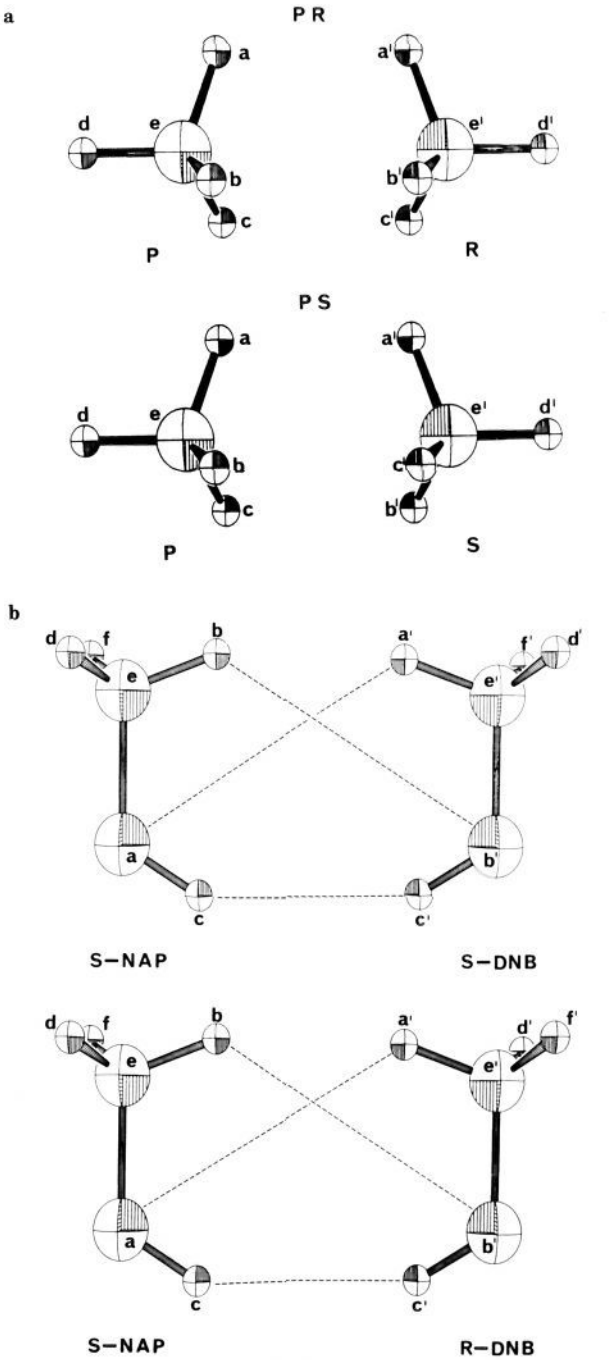

Figure 11. (a) Classical three-point model for chiral recognition. P represents a resolving agent, and R and S are two enantiomers. (b) Schematic representation of the primary interactions in the SS and SR complexes of NAP with DNB. aa′ and bb′ represent the two hydrogen bonds, and cc′ represents the $\pi-\pi$ interaction (see Figure 1).

solute–CSP complexes and are not necessary for chiral recognition".[34]

Secondly, while the interaction is repulsive, it is less repulsive for the SS complex. Again, we expect the errors in the interaction energy differences to be less than those in the total interaction energies.

Thirdly, it is possible that the inclusion of correlation effects and the use of more extensive basis sets would result in an attractive interaction energy; we are now investigating this.[35,37,38] Furthermore, results of recent studies by us show that when the structures of the complexes are optimized with the semiempirical

(30) Dagliesh, C. E. *J. Chem. Soc.* **1952**, *137*, 3940.
(31) Lipkowitz, K. B.; Demeter, D. A.; Zegarra, R.; Carter, T. *J. Am. Chem. Soc.* **1988**, *110*, 3446.
(32) Easson, L.; Stedman, E. *Biochem. J.* **1933**, *27*, 1257.
(33) Bentley, R. *Trans. N. Y. Acad. Sci.* **1983**, *41*, 5.
(34) Wainer, I. W.; Alembik, M. C. *J. Chromatogr.* **1986**, *367*, 59.

AM1 method rather than the MMFF method, the SS and SR complexes are again very similar.[35,37,38] The $\pi-\pi$ stacking region is found to have a slightly larger separation. When these AM1 structures are used to construct the PPI and PPI-SM models, the resulting interactions are stable. We anticipate that the same change will occur in the ab initio STO-3G calculations[35,37,38] and that the energy decomposition analysis will predict an increase in the relative contribution of the charge-transfer component. Nevertheless, as discussed above, it is not unreasonable to expect that the energy *differences* for the SS and SR model π complexes will not change significantly with increasing accuracy of the calculations. Moreover, we do not consider the sign of the interaction energy for the π complex model to be important because enantiomer separation can be achieved by differences in either attractive or repulsive interactions.

It is conceivable that the model of the SS complex studied herein[12] is incorrect and that, say, other intermolecular interactions are responsible for chiral separation; we are at present investigating this possibility. It should be recalled, however, that the model for the SS complex is in agreement with the experimental studies of Pirkle and Pochapsky.[12] Furthermore, the small separability factors obtained experimentally would suggest that even for a different interaction scheme, a similar analysis would hold; i.e., the SS and SR complexes would have the same primary interactions. Finally we note that formation of dimers of the *R*- and *S*-DNB analytes may compete with the formation of the complexes studied herein.[12] The observed differences in these dimers[12] may need to be considered in order to explain chiral separation and the differences in the observed spectroscopic properties of the complexes.

Conclusions

The model proposed by Pirkle and Pochapsky for the interaction of *S*-NAP with *S*- and *R*-DNB has been studied by molecular mechanics and semiempirical and ab initio quantum chemical methods. The computational studies do find a stable structure for the SS complex which is consistent with the model proposed in terms of the three primary interactions. The computational studies also find a structure for the SR complex in which the same three primary interactions are maintained. Thus enantiomer separation in these systems is not expected to be achieved via a three-point to two-point interaction mechanism but rather by through-space field effects. Such a model has recently been presented for other CSP systems.[2,31] Nevertheless, if a system would be designed in which a three-point versus two-point mechanism were responsible for chiral recognition, then one could expect significantly more efficient separation.

The π functional groups do not appear to provide any differential interactions for the SS versus SR complexes. More consistent with the findings here is that the π interaction contributes equally to the rate at which both enantiomers pass through the CSP. It may, therefore, be unnecessary to incorporate these functional groups into the design of such CSPs and the derivatization of the chiral analytes. Indeed, experimental and computational findings for analogous systems where no π interactions are possible, support this.[19,34,36]

Acknowledgment. We are grateful to K. Lipkowitz for valuable discussions and to one of the reviewers for helpful suggestions.

Registry No. NAP, 103794-11-2; D-DNB, 117096-15-8; L-DNB, 103794-12-3.

(35) Topiol, S.; Sabio, M. Computational Chemical Studies of Chiral Stationary-Phase Models: Complexes of Methyl *N*-(2-naphthyl)alaninate with *N*-(3,5-dinitrobenzoyl)leucine *n*-propylamide. *J. Chromatogr.*, in press.
(36) Hsu, T.-B.; Shah, D. A.; Rogers, L. B. *J. Chromatogr.* **1987**, *391*, 145.
(37) Sabio, M.; Topiol, S. Computational Chemical Studies of Chiral Stationary-Phase Models: The Nature of the Pi Interaction in Complexes of Methyl *N*-(2-naphthyl)alaninate with *N*-(3,5-dinitrobenzoyl)leucine *n*-propylamide. Submitted for publication.
(38) **Note Added in Proof**: Following the submission of this manuscript, we have completed studies which show that the interaction is stable at higher levels of calculation; see ref 35 and 37.

Dimensionality and Metal–Metal and Metal–Oxygen Bonding in the $NaNb_3O_6$ Structure

Maria José Calhorda† and Roald Hoffmann*

Contribution from the Department of Chemistry and Materials Science Center, Cornell University, Ithaca, New York 14853-1301. *Received April 20, 1988*

Abstract: The structures of $NaNb_3O_5F$ and $Ca_{0.75}Nb_3O_6$ were recently described. They contain NbO_3 layers built from NbO_6 distorted octahedra that share edges in one direction and corners in a perpendicular direction. These layers are held together by sodium chains and niobium chains, in which a substantial niobium–niobium bond alternation is observed. Using extended-Hückel band calculations, we explain that the niobium pair formation in the chains is the driving force for the distortions observed elsewhere in the structure. The layers must distort in order to achieve the right environment around the niobiums in the chain. In this process metal–metal bonds are also formed between niobium atoms in the chains and those in the layers, extending over the three-dimensional structure. The influence of electron count on the bonding is also discussed.

Two new niobium ternary oxides, with compositions $NaNb_3O_5F$ and $Ca_{0.75}Nb_3O_6$, were recently synthesized and structurally characterized.[1,2] The two very similar structures contain distorted octahedral Nb_6 units, in which one of the niobium–niobium bonds is extremely short. There are many oxides and halides that contain Nb metal–metal bonding pairs as, for instance, $XNbO_2$ (X = Li,[3] Na[4]), NbO_2,[5] NbI_4.[6] Higher nuclearity clusters are not unusual among niobium halides; consider the Nb_3 triangles in Nb_3I_8,[7] Nb_4 rhombuses in $CsNb_4Cl_{11}$,[8] and Nb_6 octahedra in Nb_6F_{15},[9] to cite but a few examples. On the other hand, such clusters were quite

† Permanent address: Centro de Química Estrutural, Instituto Superior Técnico, 1096 Lisboa Codex, Portugal.

(1) (a) Köhler, J.; Simon, A. *Angew. Chem., Int. Ed. Engl.* **1986**, *25*, 996. (b) Simon, A., private communication.
(2) Hibble, S. J.; Cheetham, A. K.; Cox, D. E. *Inorg. Chem.* **1987**, *26*, 2389.
(3) Meyer, G.; Hoppe, R. *J. Less Common Met.* **1976**, *46*, 55.
(4) Meyer, G.; Hoppe, R. *Z. Anorg. Allg. Chem.* **1976**, *424*, 128.
(5) Cheetham, A. K.; Rao, C. N. R. *Acta Crystallogr.* **1976**, *B32*, 1579.
(6) Dahl, L. F.; Wampler, D. L. *J. Am. Chem. Soc.* **1962**, *81*, 3150; *Acta Crystallogr.* **1962**, *15*, 903.

0002-7863/88/1510-8376$01.50/0 © 1988 American Chemical Society